JOURNAL OF THERMOPHYSICS AND HEAT TRANSFER
Vol. 17, No. 2, April–June 2003

Non-Darcy Effects on Nonparallel Thermal Instability of Horizontal Natural Convection Flow

J. Z. Zhao* and T. S. Chen†
University of Missouri-Rolla, Rolla, Missouri 65409

The non-Darcy effects on the vortex instability of natural convection flow over a horizontal flat plate embedded in a high-porosity medium are examined. These effects include the form-drag, viscous diffusion, and convective terms in the conservation equations. The instability analysis is conducted by employing the linear theory in conjunction with a nonparallel flow model, which takes into account both the streamwise and transverse variations of the disturbance amplitude functions. The resulting system of partial differential equations for the disturbance amplitude functions is converted to a system of homogeneous linear ordinary differential equations with homogeneous boundary conditions by the local nonsimilarity method. This results in an eigenvalue problem that is solved by an implicit finite difference method. The numerical results indicate that all of the three non-Darcy effects examined in the present study reduce the surface heat transfer rate as compared to the case of pure Darcy flow. These effects also render the flow to become more stable to the vortex mode of instability. Representative neutral stability curves and critical Grashof numbers are presented. It is found that the parallel flow model underpredicts the onset of thermal instability, that is, it provides lower critical Grashof numbers than the nonparallel flow model.

Nomenclature

a	=	spanwise wave number of the vortex roll
c	=	form-drag coefficient
D	=	partial derivative with respect to η
Da_x	=	Darcy number, K/x^2
Fr	=	Forchheimer number, $5^{(1-m)}c^{(2-m)}g\beta AK^{5/2}/\nu^2$
f	=	dimensionless streamfunction
Gr_x	=	local Grashof number, $g\beta[T_w(x) - T_\infty]x^3/\nu^2$
g	=	gravitational acceleration
h	=	convective heat transfer coefficient, $-k(\partial\bar{T}/\partial y)_{y=0}/[T_w(x) - T_\infty]$
K	=	Darcy permeability
k	=	thermal conductivity of porous medium; or dimensionless wave number, $ax/(Gr_x/5)^{1/5}$
m	=	exponent in the wall temperature power-law variation
Nu_x	=	local Nusselt number, hx/k
Pr	=	Prandtl number
p	=	pressure
T	=	temperature
t	=	time
u, v, w	=	streamwise, normal, and spanwise velocity components in the x, y, and z directions
x, y, z	=	streamwise, normal, and spanwise coordinates
α	=	effective thermal diffusivity
β	=	coefficient of thermal expansion
γ	=	spatial growth of the vortex roll
η	=	pseudosimilarity variable, $(y/x)(Gr_x/5)^{1/5}$
θ	=	dimensionless temperature
λ	=	ratio of volumetric heat capacity of the saturated porous medium to that of the fluid
μ	=	fluid dynamic viscosity
ν	=	fluid kinematic viscosity, μ/ρ
ξ	=	nonsimilarity parameter, $1/[Da_x(Gr_x/5)^{2/5}]$
ρ	=	fluid density
σ	=	temporal growth factor of the vortex roll
ϕ	=	porosity of the porous medium
ψ	=	stream function

Subscripts

w	=	condition at the wall
∞	=	condition at the freestream

Superscripts

$-$	=	main flow quantities
$'$	=	infinitesimal disturbance quantities
$+$	=	dimensionless disturbance quantities
$\sim$	=	amplitude of disturbance quantities
$*$	=	critical parameters

Received 5 March 2002; revision received 21 November 2002; accepted for publication 4 December 2002.

*Graduate Research Assistant, Department of Mechanical and Aerospace Engineering and Engineering Mechanics; currently Software Design Engineer, Visual-X Inc., 6615 North Big Hollow Road, Peoria, IL 61615.

†Curators' Professor Emeritus, Department of Mechanical and Aerospace Engineering and Engineering Mechanics.

I. Introduction

FOR buoyancy-inducedflows in porous media over a heated horizontal flat plate, the disturbance of flow can occur in the form of longitudinal vortex rolls. The instability of such a flow is caused by the presence of buoyancy force normal to the plate surface. Experimental investigations on thermal instability of clear fluid flow in natural convection by Sparrow and Husar[1] and by Lloyd and Sparrow[2] have shown that for inclined angles in excess of 17 deg relative to the vertical, including the horizontal case, the instability is characterized by longitudinal vortex rolls. Theoretical studies on the onset of longitudinal vortex rolls for natural convection in clear fluids have also been conducted by Hwang and Cheng,[3] Haaland and Sparrow,[4] Chen and Tzuoo,[5] and Tien et al.,[6] among others. In these analyses, a parallel flow model or quasi-parallel flow model is employed, wherein the streamwise dependence is neglected in the amplitude functions of the disturbance flow. These analyses have revealed that consideration of the nonparallelism in the base flow can affect the behavior of the neutral stability curves. Later, studies of thermal instability of natural convection flow in clear fluids conducted by Lee et al.[7,8] based on the nonparallel flow model have shown that the instability characteristics change remarkably when the nonparallelism of the disturbance amplitude functions is taken into account in the analysis.

The instability analyses of boundary-layer flows in porous media have received considerable attention in the past decades. Based on Darcy's flow model, Hsu et al.[9] and Hsu and Cheng[10] presented

instability analysis for natural convection flow over horizontal and inclined flat plates embedded in fluid-saturated porous media and solved the disturbance amplitude equations using the local similarity method by neglecting the effect of the axial variation of the amplitude functions. A similar study was carried out by Jang and Chang[11] on the thermal instability of natural convection flow over a horizontal plate in a porous medium under the combined buoyancy effects of heat and mass transfer. Later, Jang and Leu[12] also studied the effect of temperature-dependent viscosity on the thermal instability of natural convection flow over a horizontal flat plate in a porous medium.

When a high flow rate or high permeability exists in a porous medium, there is a departure from the Darcy's law, and a non-Darcy flow model should be employed in the analysis to account for the various non-Darcy effects. One well-known non-Darcy flow model is the Forchheimer model,[13] which takes into account the form-drag effect (often misleadingly referred to as the inertia effect). Another well known non-Darcy flow model is the Brinkman model,[14] which takes the viscous diffusion effect into consideration such that the flow in porous media becomes viscous flow of a clear fluid when the permeability of the porous medium is very high. A more general non-Darcy flow model includes the Forchheimer form-drag effect, the Brinkman viscous diffusion effect, and the convective effect.

The Forchheimer model was used by Chang and Jang[15] to study the form-drag effect on the vortex instability of natural convection flow over a horizontal plate. Their results have shown that the form-drag effect causes the flow to become more unstable. However, their interpretation of the form-drag term, that is, $\rho_\infty c u_i^2$ in the momentum equations, in the Forchheimer model was later questioned by Lee et al.,[16] who corrected it and studied the form-drag effect as well as the thermal dispersion effect on the thermal instability of natural convection flow along an inclined plate. Their findings have shown that, contrary to the results of Chang and Jang,[15] the form-drag term stabilizes the flow, which was also verified by Zhao and Chen[17] in a very recent sturdy based on the nonparallel flow model. Chang and Jang[18] also examined the non-Darcy effects, including the viscous diffusion effect, on the vortex instability of natural convection flow over a horizontal plate, whereas Lie and Jang[19] examined both the viscous diffusion and form-drag effects on the vortex instability of mixed convection flow for the same flow geometry. Their studies show that the viscous diffusion effect reduces the surface heat transfer rate, but it causes the flow to become more stable.

The previous investigators of the vortex instability analysis have employed the parallel or quasi-parallel flow model that assumes a weak dependence of the disturbance amplitude functions on the streamwise coordinate or the nonsimilarity parameter $\xi(x)$, that is, $\partial/\partial\xi \ll \partial/\partial\eta$, in the numerical solutions. This assumption is not consistent with the nonparallel flow model, which treats the amplitude functions of the disturbances to depend on both the x and y coordinates. The studies by Lee et al.[7,8] on thermal instability of natural convection flow in clear fluids have shown that large differences in the instability results occur between the parallel flow model and the nonparallel flow model. In addition, when compared with available experimental data, the nonparallel flow model gives more accurate instability results than the parallel flow model.

A survey of literature reveals that most of the past investigations on vortex instability of flow in porous media are inadequate because a parallel or quasi-parallel flow model is employed. To the authors' best knowledge, no investigations on vortex instability analysis seem to exist that employ the fully nonparallel flow model by considering both the x and y dependence of the disturbance amplitude functions that leads to nonsimilar equations for the disturbance amplitude functions. This has motivated the present study to reexamine the non-Darcy effects on the vortex instability of natural convection flow over a horizontal plate in a fluid-saturated porous medium by employing the nonparallel flow model. This problem was previously studied by Chang and Jang,[18] but only for the case of constant wall temperature. In addition, they did not handle the Forchheimer form-drag term properly, as was pointed out by Lee et al.,[16] and their numerical solutions were carried out under the assumption of $\partial/\partial\xi \ll \partial/\partial\eta$. That is, their results are based on the quasi-parallel flow model. In the present study, both the base flow and the disturbance flow are treated as nonparallel. In the base flow, the boundary-layer approximations are invoked, and the resulting conservation equations are transformed into a dimensionless form and then solved by an implicit finite difference method. In contrast to the work of Chang and Jang,[18] the present instability analysis is based on the nonparallel flow model using the linear theory. The resulting governing partial differential equations for the disturbance amplitude functions are converted into a system of homogeneous linear ordinary differential equations with homogeneous boundary conditions by the local nonsimilarity method. The resulting eigenvalue problem is then solved by an implicit finite difference method.

II. Analysis

The physical system considered is a semi-infinite, horizontal flat plate embedded in a porous medium, as shown in Fig. 1. The x axis is taken in the streamwise direction, the y axis is perpendicular to the plate and points outward to the porous medium, and the z axis is in the spanwise direction across the flat plate. The ambient temperature of the porous medium is uniform at T_∞, and the wall temperature is kept at a higher value, which varies as $T_w(x) = T_\infty + Ax^m$, where A and m are constants, with $A > 0$ for heating from below, as treated in the present work. To simplify the analysis, the following conventional assumptions are applied: 1) the fluid and the porous solid matrix are in local thermodynamic equilibrium under low fluid velocities; 2) the porous medium is everywhere isotropic and homogeneous; 3) the fluid properties are constant except for the density ρ in the buoyancy force term; and 4) the Boussinesq approximation is applicable. In the analysis, a general non-Darcy flow model is employed to include the form-drag effect (Forchheimer term), viscous diffusion effect (Brinkman term) and convective effect for flow in a porous medium with a high porosity. The conservation equations are

$$\nabla \cdot \boldsymbol{u} = 0 \tag{1}$$

$$\frac{\rho_\infty}{\phi^2}\boldsymbol{u}\cdot\nabla\boldsymbol{u} = -\nabla p - \frac{\mu}{K}\boldsymbol{u} - \rho_\infty c|\boldsymbol{u}|\boldsymbol{u} - \rho\boldsymbol{g} + \frac{\mu}{\phi}\nabla^2\boldsymbol{u} \tag{2}$$

$$\lambda\frac{\partial T}{\partial t} + \boldsymbol{u}\cdot\nabla T = \alpha\nabla^2 T \tag{3}$$

where $\boldsymbol{u} = (u, v, w)$ and other symbols are defined in the Nomenclature. Note that the effective viscosity in the viscous diffusion term is set equal to μ, following Brinkman,[14] and that the time derivative term involving $\partial\boldsymbol{u}/\partial t$ in Eq. (2) is dropped because in general the transients decay very rapidly.

A. Base Flow

In the present analysis, the base flow is treated within the framework of boundary-layer approximations by neglecting the higher-order terms. The general conservation equations (1–3) for steady two-dimensional laminar boundary-layer flow in natural convection in a porous medium over a horizontal flat plate can then be written as

$$\frac{\partial \bar{u}}{\partial x} + \frac{\partial \bar{v}}{\partial y} = 0 \tag{4}$$

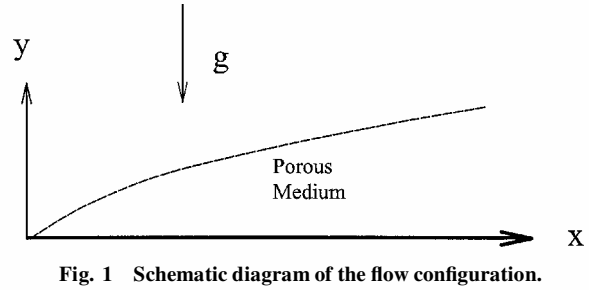

Fig. 1 Schematic diagram of the flow configuration.

$$\frac{\rho_\infty}{\phi^2}\left(\bar{u}\frac{\partial \bar{u}}{\partial x}+\bar{v}\frac{\partial \bar{u}}{\partial y}\right)=-\frac{\partial \bar{p}}{\partial x}-\frac{\mu}{K}\bar{u}-\rho_\infty c|\boldsymbol{u}|\bar{u}+\frac{\mu}{\phi}\frac{\partial^2 u}{\partial y^2} \quad (5)$$

$$0=-\frac{\partial \bar{p}}{\partial y}-\frac{\mu}{K}\bar{v}-\rho_\infty c|\boldsymbol{u}|\bar{v}-\rho g \quad (6)$$

$$\bar{u}\frac{\partial \bar{T}}{\partial x}+\bar{v}\frac{\partial \bar{T}}{\partial y}=\alpha\left(\frac{\partial^2 \bar{T}}{\partial x^2}+\frac{\partial^2 \bar{T}}{\partial y^2}\right) \quad (7)$$

When the Boussinesq approximation $\rho=\rho_\infty[1-\beta(\bar{T}-T_\infty)]$ is applied, Eq. (6) reduces to (with $\bar{v}\ll\bar{u}$)

$$0=-\frac{\partial \bar{p}}{\partial y}-\rho_\infty g[1-\beta(\bar{T}-T_\infty)]$$

$$\text{or}\quad \bar{p}_\infty-\bar{p}=-\rho_\infty g\int_y^\infty[1-\beta(\bar{T}-T_\infty)]\,dy \quad (8)$$

The pressure term in Eq. (5) induced by the buoyancy force can then be related to the temperature difference through Eq. (8) as

$$-\frac{\partial \bar{p}}{\partial x}=\rho_\infty g\beta\frac{\partial}{\partial x}\int_y^\infty(\bar{T}-T_\infty)\,dy \quad (9)$$

Next, when $-\partial\bar{p}/\partial x$ from Eq. (9) is substituted into Eq. (5) and the stream function ψ, which satisfies the mass conservation Eq. (4) with $\bar{u}=\partial\psi/\partial y$ and $\bar{v}=-\partial\psi/\partial x$, is introduced, Eqs. (5) and (7) become

$$\frac{\rho_\infty}{\phi^2}\left(\frac{\partial\psi}{\partial y}\frac{\partial^2\psi}{\partial x\partial y}-\frac{\partial\psi}{\partial x}\frac{\partial^2\psi}{\partial y^2}\right)=\rho_\infty g\beta\frac{\partial}{\partial x}\int_y^\infty(\bar{T}-T_\infty)\,dy$$

$$-\frac{\mu}{K}\frac{\partial\psi}{\partial y}-\rho_\infty c\left(\frac{\partial\psi}{\partial y}\right)^2+\frac{\mu}{\phi}\frac{\partial^3\psi}{\partial y^3} \quad (10)$$

$$\frac{\partial\psi}{\partial y}\frac{\partial\bar{T}}{\partial x}-\frac{\partial\psi}{\partial x}\frac{\partial\bar{T}}{\partial y}=\alpha\frac{\partial^2\bar{T}}{\partial y^2} \quad (11)$$

Note that, with the boundary-layer assumptions, the term $|\boldsymbol{u}|$ appearing in Eq. (5) is approximated as $|\boldsymbol{u}|=\sqrt{(\bar{u}^2+\bar{v}^2)}\approx|\bar{u}|=\bar{u}$ to arrive at Eq. (10) based on the fact that there is no recirculation region in the flow. The corresponding boundary conditions are

$$y=0:\bar{u}=0\quad\text{or}\quad\frac{\partial\psi}{\partial y}=0,\qquad\bar{v}=0\quad\text{or}\quad\frac{\partial\psi}{\partial x}=0$$

$$T_w=T_\infty+Ax^m$$

$$y\to\infty:\bar{u}=0\quad\text{or}\quad\frac{\partial\psi}{\partial y}=0,\qquad\bar{T}=T_\infty \quad (12)$$

To transform Eqs. (10–12) into a dimensionless form, the following variables are introduced:

$$\eta(x,y)=\frac{y}{x}\left(\frac{Gr_x}{5}\right)^{\frac{1}{5}},\qquad\xi(x)=\frac{1}{Da_x(Gr_x/5)^{\frac{2}{5}}}$$

$$f(\xi,\eta)=\frac{\psi(x,y)}{5\nu(Gr_x/5)^{\frac{1}{5}}},\qquad\theta(\xi,\eta)=\frac{\bar{T}-T_\infty}{T_w-T_\infty} \quad (13)$$

where $Gr_x=g\beta x^3[T_w(x)-T_\infty]/\nu^2$ is the local Grashof number and $Da_x=K/x^2$ is the local Darcy number. The transformation of Eqs. (10–12) from the (x, y) to the (ξ, η) coordinates yields the following system of equations:

$$\frac{1}{\phi}f'''+\frac{1}{\phi^2}[(m+3)ff''-(2m+1)f'^2]-\xi f'$$

$$-Fr^{1/(2-m)}\xi^{5/(4-2m)}(f')^2-\frac{m-2}{5}\eta\theta+\frac{4m+2}{5}\int_\eta^\infty\theta\,d\eta$$

$$=(4-2m)\xi\left[\frac{1}{\phi^2}f'\frac{\partial f'}{\partial\xi}-\frac{1}{\phi^2}f''\frac{\partial f}{\partial\xi}-\frac{1}{5}\frac{\partial}{\partial\xi}\int_\eta^\infty\theta\,d\eta\right] \quad (14)$$

$$\theta''+(m+3)Prf\theta'-5mPrf'\theta=(4-2m)Pr\xi\left(f'\frac{\partial\theta}{\partial\xi}-\theta'\frac{\partial f}{\partial\xi}\right) \quad (15)$$

with the boundary conditions

$$\eta=0:f'(\xi,0)=0,\qquad f(\xi,0)+\xi\frac{\partial f(\xi,0)}{\partial\xi}=0$$

$$\text{or}\qquad f(\xi,0)=0,\qquad\theta(\xi,0)=1$$

$$\eta\to\infty:f'(\xi,\infty)=0,\qquad\theta(\xi,\infty)=0 \quad (16)$$

In Eqs. (14–16) the primes denote partial differentiation with respect to η. The parameter $Fr=5^{(1-m)}c^{(2-m)}g\beta AK^{5/2}/\nu^2$ is the Forchheimer number, which expresses the relative importance of the form-drag effect. The nonsimilarity parameter ξ characterizes the local strength of the buoyancy-induced flow, Gr_x, and the permeability K of the porous medium. As x increases or $[T_w(x)-T_\infty]$ and K decrease, the value of $\xi(x)$ increases because $\xi(x)\sim x^{4/5}K^{-1}[T_w(x)-T_\infty]^{-2/5}$. Note that Darcy model corresponds to the case of $\xi\to\infty$, that is, $K\to0$, and $Fr=0$.

With the new transformation variables ξ and η, the velocity components and the local Nusselt number can be expressed as

$$\bar{u}=\frac{5\nu}{x}\left(\frac{Gr_x}{5}\right)^{\frac{2}{5}}f'$$

$$\bar{v}=-\frac{\nu}{x}\left(\frac{Gr_x}{5}\right)^{\frac{1}{5}}\left[(m+3)f+(4-2m)\xi\frac{\partial f}{\partial\xi}+(m-2)\eta f'\right]$$

$$Nu_x\left(\frac{Gr_x}{5}\right)^{-\frac{1}{5}}=-\theta'(\xi,0) \quad (17)$$

B. Disturbance Flow

The instability of the flow is analyzed based on the nonparallel flow model using the linear stability theory, in which the temperature, pressure, and velocity quantities are decomposed into the undisturbed base flow quantities and the infinitesimal disturbance quantities as

$$T(x,y,z,t)=\bar{T}(x,y)+T'(x,y,z,t)$$

$$p(x,y,z,t)=\bar{p}(x,y)+p'(x,y,z,t)$$

$$u(x,y,z,t)=\bar{u}(x,y)+u'(x,y,z,t)$$

$$v(x,y,z,t)=\bar{v}(x,y)+v'(x,y,z,t)$$

$$w(x,y,z,t)=w'(x,y,z,t) \quad (18)$$

where the overbarred and primed quantities designate, respectively, the undisturbed base flow and the disturbance flow components. It is assumed that the undisturbed base flow is a steady, two-dimensional, buoyancy-induced boundary-layer flow whose solution is governed by Eqs. (10–12) or (14–16). The disturbance flow is three dimensional.

By substituting Eq. (18) into Eqs. (1–3), subtracting the base flow quantities, and neglecting terms higher than the first order in

the disturbance quantities, the following linearized equations for the disturbance flow are obtained:

$$\frac{\partial u'}{\partial x}+\frac{\partial v'}{\partial y}+\frac{\partial w'}{\partial z}=0 \tag{19}$$

$$\frac{\rho_\infty}{\phi^2}\left[u'\frac{\partial \bar u}{\partial x}+\bar u\frac{\partial u'}{\partial x}+v'\frac{\partial \bar u}{\partial y}+\bar v\frac{\partial u'}{\partial y}\right]=-\frac{\partial p'}{\partial x}-\frac{\mu}{K}u'$$
$$-\rho_\infty c|\boldsymbol{u}|u'+\frac{\mu}{\phi}\left[\frac{\partial^2 u'}{\partial x^2}+\frac{\partial^2 u'}{\partial y^2}+\frac{\partial^2 u'}{\partial z^2}\right] \tag{20}$$

$$\frac{\rho_\infty}{\phi^2}\left[u'\frac{\partial \bar v}{\partial x}+\bar u\frac{\partial v'}{\partial x}+v'\frac{\partial \bar v}{\partial y}+\bar v\frac{\partial v'}{\partial y}\right]=-\frac{\partial p'}{\partial y}-\frac{\mu}{K}v'+\rho g\beta T'$$
$$-\rho_\infty c|\boldsymbol{u}|v'+\frac{\mu}{\phi}\left[\frac{\partial^2 v'}{\partial x^2}+\frac{\partial^2 v'}{\partial y^2}+\frac{\partial^2 v'}{\partial z^2}\right] \tag{21}$$

$$\frac{\rho_\infty}{\phi^2}\left[\bar u\frac{\partial w'}{\partial x}+\bar v\frac{\partial w'}{\partial y}\right]=-\frac{\partial p'}{\partial z}-\frac{\mu}{K}w'$$
$$-\rho_\infty c|\boldsymbol{u}|w'+\frac{\mu}{\phi}\left[\frac{\partial^2 w'}{\partial x^2}+\frac{\partial^2 w'}{\partial y^2}+\frac{\partial^2 w'}{\partial z^2}\right] \tag{22}$$

$$\lambda\frac{\partial T'}{\partial t}+\bar u\frac{\partial T'}{\partial x}+u'\frac{\partial \bar T}{\partial x}+\bar v\frac{\partial T'}{\partial y}+v'\frac{\partial \bar T}{\partial y}$$
$$=\alpha\left[\frac{\partial^2 T'}{\partial x^2}+\frac{\partial^2 T'}{\partial y^2}+\frac{\partial^2 T'}{\partial z^2}\right] \tag{23}$$

where, to linealize the disturbance quantities, the terms $|\boldsymbol{u}|u'$, $|\boldsymbol{u}|v'$, and $|\boldsymbol{u}|w'$ in Eqs. (20–22) are approximated as $\bar u u'$, $\bar u v'$, and $\bar u w'$ by letting $|\boldsymbol{u}|=\sqrt{[(\bar u+u')^2+(\bar v+v')^2+(w')^2]}\approx|\bar u|=\bar u$.

When the method of order-of-magnitude analysis described by Hsu and Cheng[10] is followed, the terms $\partial u'/\partial x$ and $\partial^2 T'/\partial x^2$ in Eqs. (19) and (23) can be neglected. The pressure terms p' in Eqs. (20–22) are eliminated by cross differentiation and subtraction. Next, the resulting equations are differentiated with respect to z, and the substitution of $\partial w'/\partial z=-\partial v'/\partial y$ from the continuity equation is employed to remove the terms involving the component w' and its derivatives. These operations lead to the following set of equations, which include only the disturbance quantities u', v', and T':

$$\frac{\rho_\infty}{\phi^2}\left[\frac{\partial^2 u'}{\partial z^2}\frac{\partial \bar u}{\partial x}+\bar u\frac{\partial^3 u'}{\partial x\partial z^2}+\frac{\partial \bar u}{\partial y}\frac{\partial^2 v'}{\partial z^2}+\bar v\frac{\partial^3 u'}{\partial y\partial z^2}+\bar u\frac{\partial^3 v'}{\partial x^2\partial y}\right.$$
$$\left.+\frac{\partial \bar u}{\partial x}\frac{\partial^2 v'}{\partial x\partial y}+\bar v\frac{\partial^3 v'}{\partial x\partial y^2}+\frac{\partial \bar v}{\partial x}\frac{\partial^2 v'}{\partial y^2}\right]=-\frac{\mu}{K}\left(\frac{\partial^2 u'}{\partial z^2}+\frac{\partial^2 v'}{\partial x\partial y}\right)$$
$$-\rho_\infty c\left(\frac{\partial \bar u}{\partial x}\frac{\partial v'}{\partial y}+\bar u\frac{\partial^2 u'}{\partial z^2}+\bar u\frac{\partial^2 v'}{\partial x\partial y}\right)$$
$$+\frac{\mu}{\phi}\left[\frac{\partial^4 u'}{\partial y^2\partial z^2}+\frac{\partial^4 u'}{\partial z^4}+\frac{\partial^4 v'}{\partial x\partial y^3}+\frac{\partial^4 v'}{\partial x\partial y\partial z^2}\right] \tag{24}$$

$$\frac{\rho_\infty}{\phi^2}\left[\frac{\partial^2 u'}{\partial z^2}\frac{\partial \bar v}{\partial x}+\bar u\frac{\partial^3 v'}{\partial x\partial z^2}+\frac{\partial \bar v}{\partial y}\frac{\partial^2 v'}{\partial z^2}+\bar v\frac{\partial^3 v'}{\partial y\partial z^2}+\bar u\frac{\partial^3 v'}{\partial x\partial y^2}\right.$$
$$\left.+\frac{\partial \bar u}{\partial y}\frac{\partial^2 v'}{\partial x\partial y}+\bar v\frac{\partial^3 v'}{\partial y^3}+\frac{\partial \bar v}{\partial y}\frac{\partial^2 v'}{\partial y^2}\right]=-\frac{\mu}{K}\left(\frac{\partial^2 v'}{\partial z^2}+\frac{\partial^2 v'}{\partial y^2}\right)$$
$$-\rho_\infty c\left(\frac{\partial \bar u}{\partial y}\frac{\partial v'}{\partial y}+\bar u\frac{\partial^2 v'}{\partial z^2}+\bar u\frac{\partial^2 v'}{\partial y^2}\right)$$
$$+\rho g\beta\frac{\partial^2 T'}{\partial z^2}+\frac{\mu}{\phi}\left[\frac{\partial^4 v'}{\partial y^2\partial z^2}+\frac{\partial^4 v'}{\partial z^4}+\frac{\partial^4 v'}{\partial y^4}+\frac{\partial^4 v'}{\partial y^2\partial z^2}\right] \tag{25}$$

$$\lambda\frac{\partial T'}{\partial t}+\bar u\frac{\partial T'}{\partial x}+u'\frac{\partial T'}{\partial x}+\bar v\frac{\partial T'}{\partial y}+v'\frac{\partial \bar T}{\partial y}=\alpha\left[\frac{\partial^2 T'}{\partial y^2}+\frac{\partial^2 T'}{\partial z^2}\right] \tag{26}$$

Next, by applying the nonparallel flow model, the three-dimensional disturbance quantities are expressed as

$$u'(x,y,z,t)=\tilde u(x,y)\cdot\exp[iaz+\sigma t+\gamma(x)]$$
$$v'(x,y,z,t)=\tilde v(x,y)\cdot\exp[iaz+\sigma t+\gamma(x)]$$
$$T'(x,y,z,t)=\tilde T(x,y)\cdot\exp[iaz+\sigma t+\gamma(x)] \tag{27}$$

where a is the spanwise periodic wave number, σ is the temporal growth factor, and $\gamma(x)=\int\alpha_i(x)\,dx$, with $\alpha_i(x)$ denoting the spatial growth factor, which is a weak function of x. Substituting Eqs. (27) into Eqs. (24–26) and setting $\sigma=\alpha_i=0$ for the stationary neutral stability condition yields

$$\frac{\rho_\infty}{\phi^2}\left[-a^2\tilde u\frac{\partial \bar u}{\partial x}-a^2\bar u\frac{\partial \tilde u}{\partial x}-a^2\tilde v\frac{\partial \bar u}{\partial y}-a^2\bar v\frac{\partial \tilde u}{\partial y}\right.$$
$$\left.+\bar u\frac{\partial^3\tilde v}{\partial x^2\partial y}+\frac{\partial \bar u}{\partial x}\frac{\partial^2\tilde v}{\partial x\partial y}+\bar v\frac{\partial^3\tilde v}{\partial x\partial y^2}+\frac{\partial \bar v}{\partial x}\frac{\partial^2\tilde v}{\partial y^2}\right]$$
$$=-\left(\frac{\mu}{K}+\rho_\infty c\bar u\right)\left(-a^2\tilde u+\frac{\partial^2\tilde v}{\partial x\partial y}\right)-\rho_\infty c\frac{\partial \bar u}{\partial x}\frac{\partial\tilde v}{\partial y}$$
$$+\frac{\mu}{\phi}\left[-a^2\frac{\partial^2\tilde u}{\partial y^2}+a^4\tilde u+\frac{\partial^4\tilde v}{\partial x\partial y^3}-a^2\frac{\partial^2\tilde v}{\partial x\partial y}\right] \tag{28}$$

$$\frac{\rho_\infty}{\phi^2}\left[-a^2\tilde u\frac{\partial \bar v}{\partial x}-a^2\bar u\frac{\partial \tilde v}{\partial x}-a^2\tilde v\frac{\partial \bar v}{\partial y}-a^2\bar v\frac{\partial \tilde v}{\partial y}+\bar u\frac{\partial^3\tilde v}{\partial x\partial y^2}\right.$$
$$\left.+\frac{\partial \bar u}{\partial y}\frac{\partial^2\tilde v}{\partial x\partial y}+\bar v\frac{\partial^3\tilde v}{\partial y^3}+\frac{\partial \bar v}{\partial y}\frac{\partial^2\tilde v}{\partial y^2}\right]$$
$$=-\left(\frac{\mu}{K}+\rho_\infty c\bar u\right)\left(-a^2\tilde v+\frac{\partial^2\tilde v}{\partial y^2}\right)-\rho_\infty c\frac{\partial \bar u}{\partial y}\frac{\partial\tilde v}{\partial y}$$
$$+\frac{\mu}{\phi}\left[-a^2\frac{\partial^2\tilde v}{\partial y^2}+a^4\tilde v+\frac{\partial^4\tilde v}{\partial y^4}-a^2\frac{\partial^2\tilde v}{\partial y^2}\right]-\rho g\beta a^2\tilde T \tag{29}$$

$$\bar u\frac{\partial\tilde T}{\partial x}+\tilde u\frac{\partial\bar T}{\partial x}+\bar v\frac{\partial\tilde T}{\partial y}+\tilde v\frac{\partial\bar T}{\partial y}=\alpha\left(\frac{\partial^2\tilde T}{\partial y^2}-a^2\tilde T\right) \tag{30}$$

with the boundary conditions

$$\tilde u=\tilde v=\tilde T=0\quad\text{at}\quad y=0\quad\text{and}\quad y\to\infty \tag{31}$$

Next, by introducing the following dimensionless quantities

$$u^+(\xi,\eta)=\frac{\tilde u x}{\nu(Gr_x/5)^{\frac{2}{5}}},\qquad v^+(\xi,\eta)=\frac{\tilde v}{5a\nu(Gr_x/5)^{\frac{1}{5}}}$$
$$\theta^+(\xi,\eta)=\frac{\tilde T}{T_w(x)-T_\infty}=\frac{\tilde T}{Ax^m},\qquad k=\frac{ax}{(Gr_x/5)^{\frac{1}{5}}} \tag{32}$$

Eqs. (28–31) can be transformed into a system of equations in dimensionless form as

$$\frac{1}{\phi}\,\mathrm{D}^2u^+ + a_1\,\mathrm{D}u^+ + a_2u^+ + a_3\frac{\partial u^+}{\partial\xi}+a_4v^+ + a_5\,\mathrm{D}v^+ + a_6\,\mathrm{D}^2v^+$$
$$+a_7\,\mathrm{D}^3v^+ + a_8\,\mathrm{D}^4v^+ + a_9\frac{\partial(Dv^+)}{\partial\xi}+a_{10}\frac{\partial(\mathrm{D}^2v^+)}{\partial\xi}$$
$$+a_{11}\frac{\partial(\mathrm{D}^3v^+)}{\partial\xi}+a_{12}\frac{\partial^2(\mathrm{D}v^+)}{\partial\xi^2}=0 \tag{33}$$

$$\frac{1}{\phi}\mathrm{D}^4v^+ + b_1\mathrm{D}^3v^+ + b_2\mathrm{D}^2v^+ + b_3\mathrm{D}v^+ + b_4v^+ + b_5\frac{\partial v^+}{\partial\xi} + b_6\frac{\partial(\mathrm{D}v^+)}{\partial\xi} + b_7\frac{\partial(\mathrm{D}^2v^+)}{\partial\xi} + b_8u^+ + b_9\theta^+ = 0 \quad (34)$$

$$\mathrm{D}^2\theta^+ + c_1\,\mathrm{D}\theta^+ + c_2\theta^+ + c_3u^+ + c_4v^+ + c_5\frac{\partial\theta^+}{\partial\xi} = 0 \quad (35)$$

with the boundary conditions

$$u^+ = v^+ = \mathrm{D}v^+ = \theta^+ = 0 \quad \text{at} \quad \eta = 0 \quad \text{and} \quad \eta\to\infty \quad (36)$$

In Eqs. (33–36), D denotes partial differentiation with respect to η and the coefficients a_n, b_n, and c_n, which are determined from the solutions of the base flow problem, are given by

$$a_1 = \frac{1}{\phi^2}[C - (m-2)\eta f']$$

$$a_2 = -\frac{k^2}{\phi} - \xi U - \frac{1}{\phi^2}[B + (2m+1)f']$$

$$a_3 = \frac{2(m-2)}{\phi}\xi f', \qquad a_4 = -\frac{25}{\phi^2}k\left(\frac{Gr_x}{5}\right)^{\frac{1}{5}} f''$$

$$a_5 = \frac{2m+1}{\phi}\frac{k}{(Gr_x/5)^{\frac{1}{5}}} + BH + (2m+1)U\frac{\xi}{k(Gr_x/5)^{\frac{1}{5}}} + \frac{2}{\phi^2}\frac{(m-2)(2m+1)}{k(Gr_x/5)^{\frac{1}{5}}}f' + \frac{2m+1}{\phi^2}\frac{B}{k(Gr_x/5)^{\frac{1}{5}}}$$

$$a_6 = \frac{m-2}{\phi}\frac{k\eta}{(Gr_x/5)^{\frac{1}{5}}} + \frac{(m-2)\eta\xi}{k(Gr_x/5)^{\frac{1}{5}}} + \frac{m-2}{\phi^2}\frac{\eta}{k(Gr_x/5)^{\frac{1}{5}}}B + \frac{5}{\phi^2}\frac{(m-1)(m-2)\eta}{k(Gr_x/5)^{\frac{1}{5}}}f' - \frac{3m-1}{\phi^2}\frac{C}{k(Gr_x/5)^{\frac{1}{5}}} - \frac{m-2}{\phi^2}\frac{E}{k(Gr_x/5)^{\frac{1}{5}}}$$

$$a_7 = -\frac{4m-3}{\phi k(Gr_x/5)^{\frac{1}{5}}} - \frac{1}{\phi^2}\frac{(m-2)^2\eta^2}{k(Gr_x/5)^{\frac{1}{5}}}f' - \frac{(m-2)\eta}{\phi^2k(Gr_x/5)^{\frac{1}{5}}}C$$

$$a_8 = -\frac{m-2}{\phi}\frac{\eta}{k(Gr_x/5)^{\frac{1}{5}}}$$

$$a_9 = (4-2m)\xi\left[\frac{1}{\phi}\frac{k}{(Gr_x/5)^{\frac{1}{5}}} + \frac{\xi U}{k(Gr_x/5)^{\frac{1}{5}}}\right] - \frac{2}{\phi^2}\frac{(m-2)(2m+1)\xi}{k(Gr_x/5)^{\frac{1}{5}}}f' + \frac{4-2m}{\phi^2}\frac{\xi B}{k(Gr_x/5)^{\frac{1}{5}}}$$

$$a_{10} = -\frac{4}{\phi^2}\frac{(m-2)^2\eta\xi}{k(Gr_x/5)^{\frac{1}{5}}}f' - \frac{4-2m}{\phi^2}\frac{\xi}{k(Gr_x/5)^{\frac{1}{5}}}C$$

$$a_{11} = -\frac{4-2m}{\phi}\frac{\xi}{k(Gr_x/5)^{\frac{1}{5}}}, \qquad a_{12} = \frac{4}{\phi^2}\frac{(m-2)^2\xi^2}{k(Gr_x/5)^{\frac{1}{5}}}f'$$

$$b_1 = \frac{1}{\phi^2}\left[(m+3)f + (4-2m)\xi\frac{\partial f}{\partial\xi}\right]$$

$$b_2 = -\frac{2}{\phi}k^2 - \xi U + \frac{2-m}{\phi^2}\left[f' + 2\xi\frac{\partial f'}{\partial\xi}\right]$$

$$b_3 = -Gf'' - \frac{k^2}{\phi^2}\left[(m+3)f - 2(m-2)\xi\frac{\partial f}{\partial\xi}\right] - \frac{2m+1}{\phi^2}f''$$

$$b_4 = \frac{k^4}{\phi} + \xi k^2U + \frac{2-m}{\phi^2}k^2\left[f' + \eta f'' - 2\xi\frac{\partial f'}{\partial\xi}\right]$$

$$b_5 = \frac{4-2m}{\phi^2}\xi k^2 f', \qquad b_6 = -\frac{4-2m}{\phi^2}\xi f''$$

$$b_7 = -\frac{4-2m}{\phi^2}\xi f', \qquad b_8 = -\frac{m-2}{25\phi^2}\frac{kE}{(Gr_x/5)^{\frac{1}{5}}}$$

$$b_9 = -k\left(\frac{Gr_x}{5}\right)^{\frac{1}{5}}$$

$$c_1 = Pr\left[(m+3)f + (4-2m)\xi\frac{\partial f}{\partial\xi}\right], \qquad c_2 = -(k^2 + 5mPrf')$$

$$c_3 = -Pr\cdot F, \qquad c_4 = -5kPr\left(\frac{Gr_x}{5}\right)^{\frac{1}{5}}\theta'$$

$$c_5 = -(4-2m)Pr\xi f' \quad (37)$$

In Eq. (37), the expressions for B, C, E, F, G, H, and U are

$$B = (2m+1)f' + (m-2)\eta f'' + (4-2m)\xi\frac{\partial f'}{\partial\xi}$$

$$C = (m+3)f + (m-2)\eta f' + (4-2m)\xi\frac{\partial f}{\partial\xi}$$

$$E = (m+3)f + (3m-1)\eta f' + (m-2)\eta^2 f'' - 10\xi\frac{\partial f}{\partial\xi} + 4(m-2)\xi^2\frac{\partial^2 f}{\partial\xi^2} - 4(m-2)\eta\xi\frac{\partial f'}{\partial\xi}$$

$$F = m\theta + \frac{m-2}{5}\eta\theta' + \frac{4-2m}{5}\xi\frac{\partial\theta}{\partial\xi}$$

$$G = Fr^{1/(2-m)}\xi^{5/(4-2m)}, \qquad H = \frac{G}{k(Gr_x/5)^{\frac{1}{5}}}$$

$$U = 1 + \frac{\rho_\infty cK}{\mu}\bar{u} = 1 + \frac{5cx}{\xi}f' = 1 + Fr^{1/(2-m)}\xi^{(1+2m)/(4-2m)}f' \quad (38)$$

Equations (33–35), along with the boundary conditions (36), constitute the mathematical system for the flow instability problem. They are coupled parabolic partial differential equations, but the boundary conditions are not sufficient to give any initial profile at a certain ξ_0 position. Therefore, the commonly used "marching method" for parabolic partial differential equations can not be employed to obtain the complete solution. Two solution methods are generally employed to solve such a system of equations: the local similarity approximation and the local nonsimilarity approximation. With the local similarity approximation, the amplitude functions of the disturbances are assumed to have a weak dependence in the streamwise direction, that is, $\partial/\partial\xi \ll \partial/\partial\eta$, and all terms involving the derivative with respect to ξ are neglected. This approach is the local similarity method and corresponds to the quasi-parallel flow model. The system of partial differential equations (33–35) are then reduced to a set of ordinary differential equations, whose solution can be obtained with the boundary conditions (36).

To apply the fully nonparallel flow model in the instability analysis, the local nonsimilarity solution method should be employed. In the solution by the local nonsimilarity method, all terms in Eqs. (33–35) are retained. Next, Eqs. (33–35), as well as the boundary conditions (36), are differentiated with respect to ξ to give three additional partial differential equations for $\partial u^+/\partial\xi$, $\partial v^+/\partial\xi$, and $\partial\theta^+/\partial\xi$, along with the corresponding additional boundary conditions. To obtain the next higher order of equations for $\partial^2u^+/\partial\xi^2$,

$\partial^2 v^+/\partial\xi^2$, and $\partial^2\theta^+/\partial\xi^2$, the resulting differential equations and boundary conditions for $\partial u^+/\partial\xi$, $\partial v^+/\partial\xi$, and $\partial\theta^+/\partial\xi$ are differentiated again with respect to ξ. For the third level of truncation, all of the terms involving the third-order partial derivative with respect to ξ, such as $\partial^3 u^+/\partial\xi^3$, $\partial^3 v^+/\partial\xi^3$, and $\partial^3\theta^+/\partial\xi^3$, are neglected in the resulting equations and boundary conditions. This operation leads to the following system of equations and boundary conditions for $u^+, v^+, \theta^+, \delta = \partial u^+/\partial\xi, \sigma = \partial v^+/\partial\xi, \omega = \partial\theta^+/\partial\xi, q = \partial^2 u^+/\partial\xi^2$, $g = \partial^2 v^+/\partial\xi^2$, and $h = \partial^2\theta^+/\partial\xi^2$:

$$(1/\phi)\,\mathrm{D}^2u^+ + a_1\,\mathrm{D}u^+ + a_2u^+ + a_3\delta + a_4v^+ + a_5\,\mathrm{D}v^+ + a_6\,\mathrm{D}^2v^+ + a_7\,\mathrm{D}^3v^+ + a_8\,\mathrm{D}^4v^+ + a_9\,\mathrm{D}\sigma + a_{10}\,\mathrm{D}^2\sigma + a_{11}\,\mathrm{D}^3\sigma + a_{12}\,\mathrm{D}g = 0$$

$$(1/\phi)\,\mathrm{D}^4v^+ + b_1\,\mathrm{D}^3v^+ + b_2\,\mathrm{D}^2v^+ + b_3\,\mathrm{D}v^+ + b_4v^+ + b_5\sigma + b_6\,\mathrm{D}\sigma + b_7\,\mathrm{D}^2\sigma + b_8u^+ + b_9\theta^+ = 0$$

$$\mathrm{D}^2\theta^+ + c_1\,\mathrm{D}\theta^+ + c_2\theta^+ + c_3u^+ + c_4v^+ + c_5\omega = 0$$

$$(1/\phi^2)\,\mathrm{D}^2\delta + d_1\,\mathrm{D}\delta + d_2\delta + d_3u^+ + d_4\,\mathrm{D}u^+ + d_5v^+ + d_6\,\mathrm{D}v^+ + d_7\,\mathrm{D}^2v^+ + d_8\,\mathrm{D}^3v^+ + d_9\,\mathrm{D}^4v^+ + d_{10}q + d_{11}\sigma + d_{12}\,\mathrm{D}\sigma + d_{13}\,\mathrm{D}^2\sigma + d_{14}\,\mathrm{D}^3\sigma + d_{15}\,\mathrm{D}^4\sigma + d_{16}\,\mathrm{D}g + d_{17}\,\mathrm{D}^2g + d_{18}\,\mathrm{D}^3g = 0$$

$$(1/\phi)\,\mathrm{D}^4\sigma + e_1\,\mathrm{D}^3\sigma + e_2\,\mathrm{D}^2\sigma + e_3\,\mathrm{D}\sigma + e_4\sigma + e_5u^+ + e_6\theta^+ + e_7v^+ + e_8\,\mathrm{D}v^+ + e_9\,\mathrm{D}^2v^+ + e_{10}\,\mathrm{D}^3v^+ + e_{11}\delta + e_{12}g + e_{13}\,\mathrm{D}g + e_{14}\,\mathrm{D}^2g + e_{15}\omega = 0$$

$$\mathrm{D}^2\omega + f_1\,\mathrm{D}\omega + f_2\omega + f_3\theta^+ + f_4\,\mathrm{D}\theta^+ + f_5v^+ + f_6\delta + f_7\sigma + f_8u^+ + f_9h = 0$$

$$(1/\phi)\,\mathrm{D}^2q + l_1\,\mathrm{D}q + l_2q + l_3u^+ + l_4\,\mathrm{D}u^+ + l_5\delta + l_6\,\mathrm{D}\delta + l_7v^+ + l_8\,\mathrm{D}v^+ + l_9\,\mathrm{D}^2v^+ + l_{10}\,\mathrm{D}^3v^+ + l_{11}\,\mathrm{D}^4v^+ + l_{12}\sigma + l_{13}\,\mathrm{D}\sigma + l_{14}\,\mathrm{D}^2\sigma + l_{15}\,\mathrm{D}^3\sigma + l_{16}\,\mathrm{D}^4\sigma + l_{17}g + l_{18}\,\mathrm{D}g + l_{19}\,\mathrm{D}^2g + l_{20}\,\mathrm{D}^3g + l_{21}\,\mathrm{D}^4g$$

$$(1/\phi)\,\mathrm{D}^4g + m_1\,\mathrm{D}^3g + m_2\,\mathrm{D}^2g + m_3\,\mathrm{D}g + m_4g + m_5v^+ + m_6\,\mathrm{D}v^+ + m_7\,\mathrm{D}^2v^+ + m_8\,\mathrm{D}^3v^+ + m_9\sigma + m_{10}\,\mathrm{D}\sigma + m_{11}\,\mathrm{D}^2\sigma + m_{12}\,\mathrm{D}^3\sigma + m_{13}u^+ + m_{14}\delta + m_{15}q + m_{16}\theta^+ + m_{17}\omega + m_{18}h = 0$$

$$\mathrm{D}^2h + n_1\,\mathrm{D}h + n_2h + n_3\omega + n_4\,\mathrm{D}\omega + n_5\theta^+ + n_6D\theta^+ + n_7u^+ + n_8\delta + n_9q + n_{10}v^+ + n_{11}\sigma + n_{12}g = 0 \qquad (39)$$

with the boundary conditions

$$u^+ = v^+ = \mathrm{D}v^+ = \theta^+ = \delta = \sigma = \mathrm{D}\sigma = \omega = q = g = \mathrm{D}g = h = 0 \quad \text{at} \quad \eta = 0 \quad \text{and} \quad \eta \to \infty \qquad (40)$$

In Eq. (39), the coefficients a_n, b_n, and c_n are as given in Eq. (37). However, to conserve space, the coefficients d_n, e_n, f_n, l_n, m_n, and n_n are not presented. They are available elsewhere.[20]

The set of coupled homogeneous linear ordinary differential equations (39), along with the homogeneous boundary conditions (40), constitutes a closed form of the mathematical system for the instability problem, which is an eigenvalue problem of the form

$$E(Gr_x, k; Pr, m, \phi, Fr, \xi) = 0 \qquad (41)$$

In the determination of the neutral stability curve for given values of wall temperature exponent m, Prandtl number Pr, medium porosity ϕ, Forchheimer number Fr, and local Darcy number Da_x or nonsimilarity parameter ξ, the value of wave number k satisfying Eq. (41) is sought as the eigenvalue for a prescribed value of Grashof number Gr_x.

III. Numerical Method of Solutions

The system of Eqs. (14–16) for the base flow are solved by an efficient and accurate implicit finite difference method that is similar to that described by Cebeci and Bradshaw.[21] Along with the use of a cubic spline interpolation procedure, the base flow solutions provide the base flow quantities f, f', f'', θ, θ', and their partial derivatives with respect to ξ, which are required in the flow instability calculations.

The instability problem, which is described by the system of coupled homogeneous linear ordinary differential equations (39), with homogeneous boundary conditions (40), can also be solved with the similar implicit finite difference method. It suffices to mention the highlights of the eigenvalue problem. With a preassigned value of the nonsimilarity parameter $\xi = 1/[Da_x(Gr_x/5)^{2/5}]$, the base flow solution is first obtained for fixed Prandtl number Pr, Forchheimer number Fr, medium porosity ϕ, and wall temperature variation exponent m. Next, with a guessed value of wave number k as the eigenvalue and a nonzero value boundary condition $[\mathrm{D}^2v^+(\xi, 0) = 1]$ as the normalizing condition, the eigenvalue problem is solved for a fixed Grashof number Gr_x. The guessed eigenvalue k is then adjusted by the Newton–Raphson differential-correction iterative scheme until all the boundary conditions at the wall ($\eta = 0$) are satisfied within a certain specified tolerance ($\varepsilon = 1 \times e{-}6$). This yields a converged value of k for given values of m, Pr, ϕ, Fr, Gr_x, and ξ.

In the numerical calculations, a step size of $\Delta\xi = 0.01$ was used and found to give accurate results for both the base flow and the disturbance flow. Note that a larger step size $\Delta\xi$ can be used in the solution of the base flow when the values of ξ are very large, so that the computation time can be saved. In the η direction, $\Delta\eta = 0.01$ was found sufficient to give accurate results in both the base flow calculations and the instability calculations for any Prandtl number. The value of boundary-layer thickness η_∞ was set to 10.0 for $\xi < 10$, but a larger value of η_∞ was required to obtain convergent solutions for a larger value of ξ ($\eta_\infty = 15$ for $\xi = 30$ and $\eta_\infty = 20$ for $\xi = 50$) because of the increasing boundary-layer thickness.

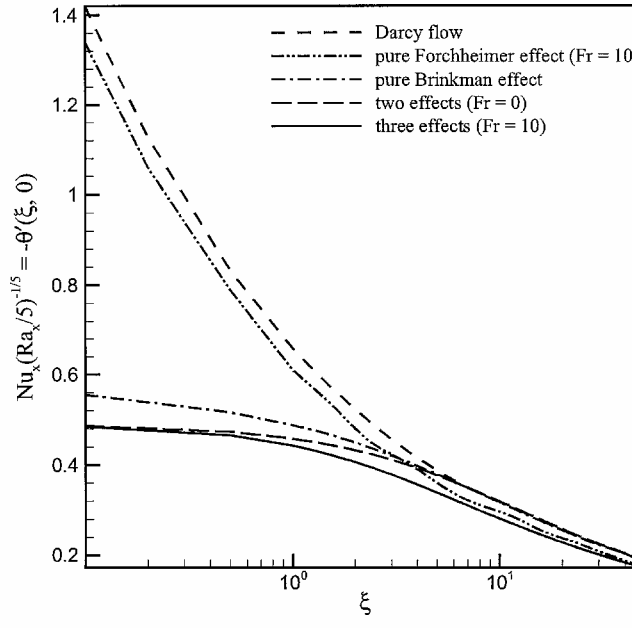

Fig. 2 Local Nusselt number vs ξ for Darcy flow and non-Darcy flows, $m = 0$.

IV. Results and Discussion

Representative numerical results are presented for the cases of $m = 0$, which corresponds to the constant wall temperature condition, and $m = \frac{1}{3}$, which corresponds approximately to the constant wall heat flux condition, because $q_w(x) = -k(\partial T/\partial y)_{y=0} = -k(T_w - T_\infty)\theta'(\xi, 0)(Gr_x/5)^{1/5}/x \propto x^{2(3m-1)/5}\theta'(\xi, 0)$. Moreover, the Prandtl number Pr and medium porosity ϕ are set to be 0.72 and 0.98, respectively.

The velocity and temperature distributions across the boundary layer in the base flow are omitted here because they are similar to those shown by Chang and Jang.[18] Only the local Nusselt number variation with ξ, or the dimensionless surface temperature gradient, $-\theta'(\xi, 0)$, is shown in Fig. 2 for the case of constant wall temperature, that is, $m = 0$. Figure 2 shows clearly the different non-Darcy effects on the local surface heat transfer rate. The three non-Darcy effects (convective effect, Brinkman viscous diffusion effect, and Forchheimer form-drag effect) all tend to reduce the heat transfer rate at the wall. It is seen that both the Darcy model and the Forchheimer non-Darcy model, that is, only the form-drag effect is considered, overpredict the heat transfer rate at the wall when ξ is small and are valid only for large values of ξ ($\xi > 10$). Based on a comparison of results between the case of pure Brinkman viscous diffusion effect and the case of two effects (with both the Brinkman viscous diffusion effect and the convective effect, but without the Forchheimer form-drag effect), the convective effect is seen to become important when $\xi < 3$. Moreover, from a comparison between the results from solutions of the two effects (with $Fr = 0$) and three effects (with $Fr = 10$), it is seen that the form-drag effect becomes significant when the value of ξ is larger than 0.5.

Figures 3a and 3b show the neutral stability curves (Gr_x vs k curves) for Darcy flow and non-Darcy flows (two effects with $Fr = 0$ and three effects with $Fr = 10$) for $\xi = 10$ and $m = 0$ and $\frac{1}{3}$, respectively. Solutions from the parallel flow model and the nonparallel flow model are shown in both figures for comparisons. It can be seen that a large discrepancy in the instability results exists between the parallel flow model and the nonparallel flow model. It is noted that a neutral stability curve separates the unstable flow domain (above the curve) from the stable flow domain (below the curve). Thus, the flow is unstable when a pair of (Gr_x, k) lies above the curve, and the flow is stable when it lies below the curve. The minimum Gr_x value on a neutral stability curve is the critical Grashof number Gr_x^*, with a corresponding wave number k^*, which signifies the onset of the instability of flow. The parallel flow model underpredicts the critical Grashof number Gr_x^* as compared to the nonparallel flow model. This means that the dependence of the disturbance amplitudes on the streamwise coordinate (that is, x or ξ) cannot be neglected in the instability analysis because the ξ-dependent disturbance terms neglected in the parallel flow model have a great stabilizing effect. In both Figs. 3a and 3b, the non-Darcy effects are seen to shift the neutral stability curves upward as compared to the case of Darcy flow, which indicates that all of the non-Darcy effects examined here contribute to the stabilization of the flow to the vortex mode of instability. Furthermore, a comparison between the two effects (with $Fr = 0$) and three effects (with $Fr = 10$) indicates that the form-drag effect causes the flow to become more stable.

Figures 4a and 4b show a comparison of the neutral stability curves for selected values of m(0 and 1/3) for non-Darcy flows, respectively, for two effects with $Fr = 0$ and three effects with $Fr = 10$. It is seen from Figs. 4a and 4b that $m = 0$ (that is, the constant wall temperature case) represents the most unstable flow situation and that a flow with a larger value of m is less susceptible

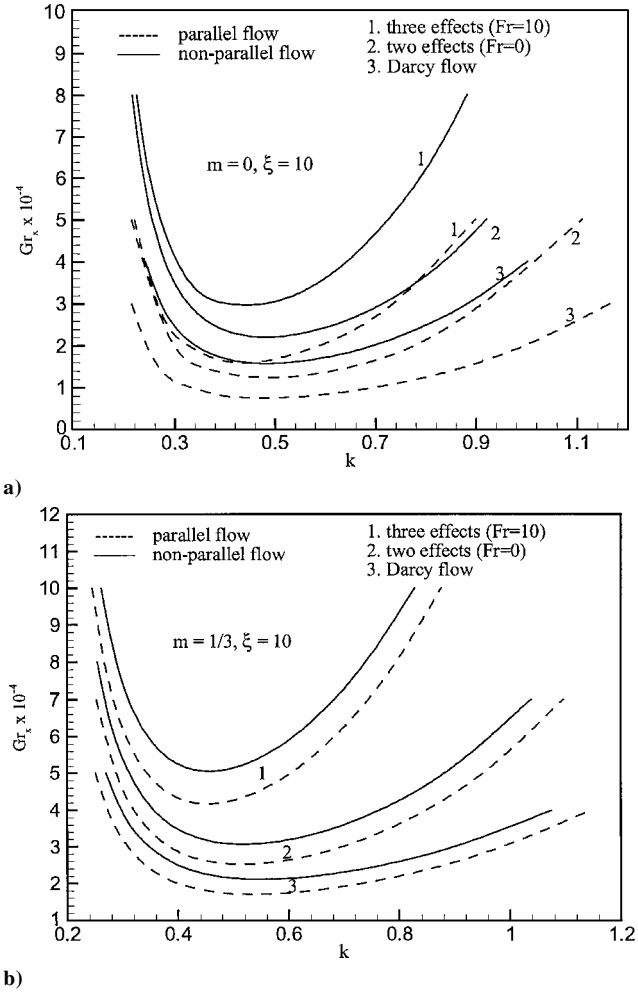

Fig. 3 Neutral stability curves for different cases, ξ = 10. a) m = 0 and b) m = 1/3.

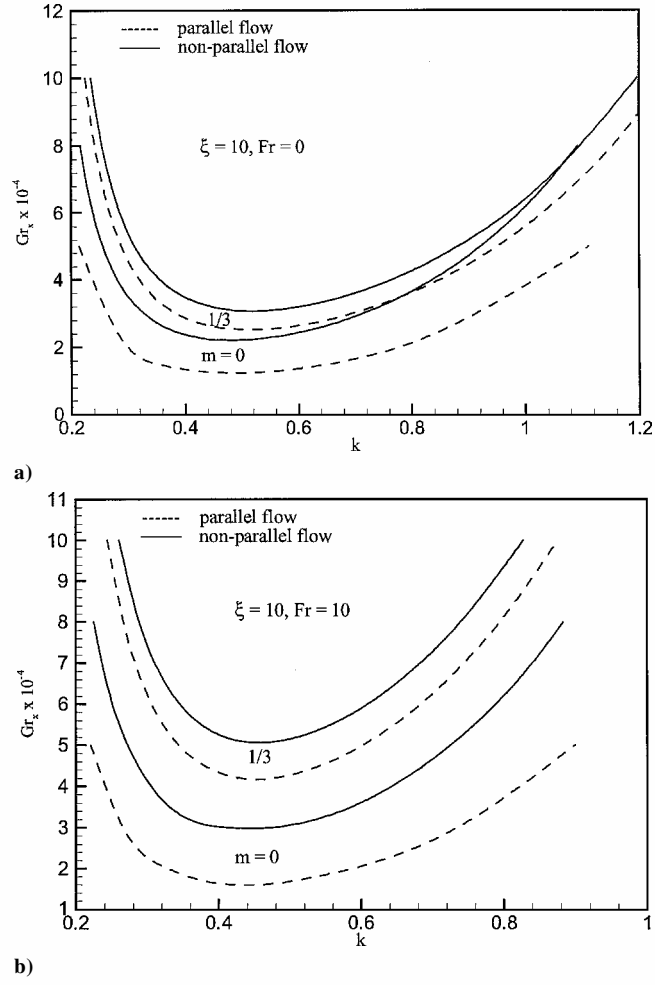

Fig. 4 Neutral stability curves for selected values of m, ξ = 10. a) $Fr = 0$ and b) Fr = 10.

Table 1 Critical Grashof numbers Gr_x^* for Darcy flow and non-Darcy flows, $m = 0$

		Two effects ($Fr = 0$)		Three effects ($Fr = 10$)	
ξ	Darcy flow	Parallel flow	Nonparallel flow	Parallel flow	Nonparallel flow
0.1	4.4	1,154.4	2,983.5	1,157.3	2,983.6
0.5	64.6	1,375.9	3,189.3	1,414.3	3,257.3
1.0	205.3	1,690.75	3,652.0	1,820.7	3,853.8
5.0	3,001.9	5,258.9	9,858.6	6,674.1	12,524.2
10.0	9,530.7	12,394.4	22,087.3	15,912.7	29,840.9
20.0	30,258.1	30,886.7	59,007.6	37,518.5	77,972.3
30.0	59,474.0	56,464.2	109,728.1	71,964.9	142,693.1
40.0	96,063.5	86,604.9	166,474.3	112,462.3	222,703.3
50.0	139,339.8	123,617.1	248,874.1	154,982.1	308,776.1

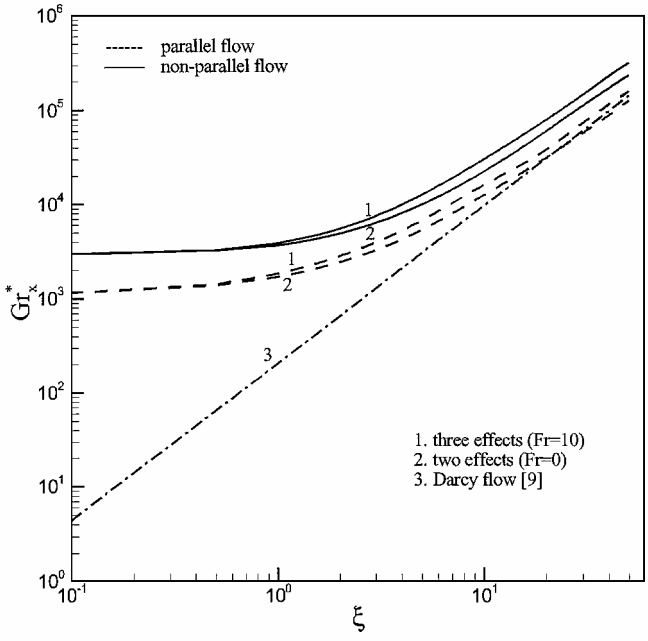

Fig. 5 Comparison of the critical Grashof numbers between Darcy flow and non-Darcy flows, $m = 0$.

to the vortex mode of instability. This is because the case of $m = 0$ corresponds to a step change in the wall temperature, which indicates a heating condition that causes the flow to be more susceptible to thermal instability than the case of $m = \frac{1}{3}$, which has a slower rate of increase in the wall temperature along the plate.

The critical Grashof numbers Gr_x^*, which mark the onset of longitudinal vortex rolls, are shown in Fig. 5 for Darcy flow and non-Darcy flows with two effects (with $Fr = 0$) and three effects (with $Fr = 10$). The result for Darcy flow is taken from the work of Hsu et al.[9] A comparison of the results between the parallel flow model and the nonparallel flow model for the non-Darcy flow is also made in Fig. 5. For completeness, all critical Grashof number (Gr_x^*) results are listed in Table 1. It can be seen clearly from Fig. 5 and Table 1 that the parallel flow model always predicts a lower critical Grashof number for any value of ξ. When Darcy flow and non-Darcy flow are compared, it is seen that all of the non-Darcy effects (convective, viscous diffusion, and form-drag effects) contribute to stabilization of the flow. The Darcy model greatly underpredicts the onset of longitudinal vortex rolls when the value of ξ is small (such as flow in a porous medium with high permeability). The discrepancy in the Gr_x^* values between the Darcy flow and non-Darcy flow decreases with increasing value of ξ. In addition, a comparison of the Gr_x^* results between the two effects (with $Fr = 0$) and three effects (with $Fr = 10$) indicates again that the form-drag effect has a stabilizing effect on the flow, but it can be neglected when the value of ξ is small ($\xi < 0.6$). It is noted from Fig. 5 that for large ξ values the curve for the three effects (with $Fr = 10$) lies above the curve for Darcy flow. In contrast, the curve for the three effects given by Chang and Jang[18] lies below the curve for Darcy flow; that is, their analysis has predicted lower critical Grashof numbers in the presence of form-drag effects.

V. Conclusions

The non-Darcy effects (convective, viscous diffusion, and form-drag effects) on the vortex instability of natural convection flow in a fluid-saturated porous medium over a horizontal plate are analyzed using the linear theory in conjunction with the nonparallel flow model. The resulting system of coupled parabolic differential equations for the disturbance amplitude functions in dimensionless form are converted into a system of homogeneous linear ordinary differential equations with homogeneous boundary conditions by the local nonsimilarity method. The resulting eigenvalue problem is then solved by an implicit finite difference method. The major findings from the present study are as follows. 1) The convective, viscous diffusion and form-drag effects all reduce the heat transfer rate at the wall and contribute to stabilization of the flow to the vortex mode of instability. 2) The parallel flow model underpredicts the onset of thermal instability as compared to the nonparallel flow model. 3) It is more appropriate to employ the nonparallel flow model in the vortex instability analysis than the parallel or quasi-parallel flow model.

References

[1]Sparrow, E. M., and Husar, R. B., "Longitudinal Vortices in Natural Convection Flow on Inclined Plates," *Journal of Fluid Mechanics*, Vol. 37, Pt. 2, 1969, pp. 251–255.

[2]Lloyd, J. R., and Sparrow, E. M., "On the Instability of Natural Convection Flow on Inclined Plates," *Journal of Fluid Mechanics*, Vol. 42, Pt. 3, 1970, pp. 465–470.

[3]Hwang, G. J., and Cheng, K. C., "Thermal Instability of Laminar Natural Convection Flow on Inclined Isothermal Plates," *Canadian Journal of Chemical Engineering*, Vol. 51, No. 6, 1973, pp. 659–666.

[4]Haaland, S. E., and Sparrow, E. M., "Vortex Instability of Natural Convection Flow on Inclined Surfaces," *International Journal of Heat and Mass Transfer*, Vol. 16, No. 12, 1973, pp. 2355–2367.

[5]Chen, T. S., and Tzuoo, K. L., "Vortex Instability of Free Convection Flow over Horizontal and Inclined Surfaces," *Journal of Heat Transfer*, Vol. 104, No. 4, 1982, pp. 637–643.

[6]Tien, H. C., Chen, T. S., and Armaly, B. F., "Vortex Instability of Natural Convection Flow over Horizontal and Inclined Plates with Uniform Surface Heat Flux," *Numerical Heat Transfer*, Vol. 9, No. 6, 1986, pp. 697–713.

[7]Lee, H. R., Chen, T. S., and Armaly, B. F., "Nonparallel Vortex Instability of Natural Convection Flow over a Nonisothermal Horizontal Flat Plate," *International Journal of Heat and Mass Transfer*, Vol. 34, No. 1, 1991, pp. 305–313.

[8]Lee, H. R., Chen, T. S., and Armaly, B. F., "Nonparallel Thermal Instability of Natural Convection Flow on Nonisothermal Inclined Flat Plates," *International Journal of Heat and Mass Transfer*, Vol. 35, No. 1, 1992, pp. 207–220.

[9]Hsu, C. T., Cheng, P., and Homsy, G. M., "Instability of Free Convection Flow over a Horizontal Impermeable Surface in a Porous Medium," *International Journal of Heat and Mass Transfer*, Vol. 21, No. 9, 1978, pp. 1221–1228.

[10]Hsu, C. T., and Cheng, P., "Vortex Instability of Buoyancy-Induced Flow over Inclined Heated Surfaces in Porous Media," *Journal of Heat Transfer*, Vol. 101, No. 4, 1979, pp. 660–665.

[11] Jang, J. Y., and Chang, W. J., "The Flow and Vortex Instability of Horizontal Natural Convection in a Porous Medium Resulting from Combined Heat and Mass Buoyancy Effects," *International Journal of Heat and Mass Transfer*, Vol. 31, No. 4, 1988, pp. 769–777.

[12] Jang, J. Y., and Leu, J. S., "Variable Viscosity Effects on the Vortex Instability of Free Convection Boundary Layer Flow over a Horizontal Surface in a Porous Medium," *International Journal of Heat and Mass Transfer*, Vol. 36, No. 5, 1993, pp. 1287–1294.

[13] Forchheimer, P., "Wasserbewegung Durch Bodeu," *Zeitschrift des Vereines Deutscher Ingenieure*, Vol. 45, 1901, pp. 1736–1741, 1781–1788.

[14] Brinkman, H. C., "A Calculation of the Viscous Force Exerted by a Flowing Fluid on a Dense Swarm of Particles," *Applied Scientific Research*, Vol. A1, 1947, pp. 27–34.

[15] Chang, W. J., and Jang, J. Y., "Inertia Effects on Vortex Instability of a Horizontal Natural Convection Flow in a Saturated Porous Medium," *International Journal of Heat and Mass Transfer*, Vol. 32, No. 3, 1989, pp. 541–550.

[16] Lee, D. H., Yoon, D. Y., and Choi, C. K., "The Onset of Vortex Instability in Laminar Natural Convection Flow over an Inclined Plate Embedded in a Porous Medium," *International Journal of Heat and Mass Transfer*, Vol. 43, No. 16, 2000, pp. 2895–2908.

[17] Zhao, J. Z., and Chen, T. S., "Inertia Effects on Nonparallel Thermal Instability of Natural Convection Flow over Horizontal and Inclined Plates in Porous Media," *International Journal of Heat and Mass Transfer*, Vol. 45, No. 11, 2002, pp. 2265–2276.

[18] Chang, W. J., and Jang, J. Y., "Non-Darcian Effects on Vortex Instability of a Horizontal Natural Convection Flow in a Porous Medium," *International Journal of Heat and Mass Transfer*, Vol. 32, No. 3, 1989, pp. 529–539.

[19] Lie, K. N., and Jang, J. Y., "Boundary and Inertia Effects on Vortex Instability of a Horizontal Mixed Convection Flow in a Porous Medium," *Numerical Heat Transfer*, Pt. A, Vol. 23, No. 3, 1993, pp. 361–378.

[20] Zhao, J. Z., "Nonparallel Thermal Instability of Natural Convection Flow over Inclined Plates in Porous Media," Ph.D. Dissertation (Sec. 3), Dept. of Mechanical and Aerospace Engineering and Engineering Mechanics, Univ. of Missouri, Rolla, MO, May 2001.

[21] Cebeci, T., and Bradshaw, P., *Physical and Computational Aspects of Convective Heat Transfer*, Springer-Verlag, New York, 1984, Chap. 13.